

Distinguishability theory for multiphoton interference with time-resolved photodetection and boson sampling

V. S. Shchesnovich and M. E. O. Bezerra

Centro de Ciências Naturais e Humanas, Universidade Federal do ABC, Santo André, SP, 09210-170 Brazil

We consider possible experimental realization of boson sampling with single photons when fast detectors, capable of precise resolution of photon arrival time, are employed and investigate if such a photodetection allows to circumvent distinguishability of realistic single photons in mixed states. To this goal, we compare the effect of distinguishability of photons in two setups of experimental boson sampling: (a) with photons in the same average (temporal) profile on a spatial interferometer and photodetection incapable of (or with strongly imprecise) time resolution and (b) with photons in generally different average temporal profiles on the same spatial interferometer and photodetection with precise time resolution. Exact analytical results are obtained for Gaussian single photons of different central frequencies with Gaussian distribution of arrival times. We find that distinguishability of photons in the two setups is strikingly similar. For the same purity of photon states, only the same quality experimental boson sampling can be achieved using either of the two considered setups. The upshot of our results is that distinguishability due to mixed states is an intrinsic property of photons, whatever the photodetection scheme.

PACS numbers: 42.50.St, 03.67.Ac, 42.50.Ar

I. INTRODUCTION

We have witnessed enormous experimental progress [1] towards demonstration of quantum advantage over classical computations with boson sampling [2]. Recent experiment with 20 single input photons on a 60-mode interferometer [3] is a big step towards the ultimate goal of demonstrating the quantum advantage. For such a quantum device, scaled up beyond possibility to exhaust all outputs in an experiment, it is of paramount importance to establish to what extent the quantum advantage survives sources of noise/imperfections of an experimental setup and whether one could circumvent at least some imperfections in some way. One important source of noise/imperfection is, of course, photon distinguishability [4], having exponentially strong effect with the number of photons [5–7] and leading to efficient simulation of experimental boson sampling on digital computers [8]. Besides distinguishability of photons, there are many other sources of noise/imperfections affecting optical boson sampling devices, such as noise in interferometer [9–11], photon losses and random counts of detectors [12–14]. The quality of an experimental boson sampling device will depend on all such sources of noise, recently shown to satisfy equivalence relations [15].

With respect to distinguishability of photons in a large-scale multiphoton interference experiment, such as boson sampling with single photons, notwithstanding many theoretical and experimental results [6, 16–28], there still remains an issue lacking a detailed investigation. Namely, to what extent it is possible to circumvent the distinguishability by using photodetection capable of resolution of internal states of photons, for instance, by photodetection with precise resolution in time (i.e., by using fast detectors as compared to photon pulse duration). It was previously suggested [21, 23] that such time-resolved photodetection allows to change partial distinguishability

of photons, though the result is limited to only pure-state distinguishability.

In this work we investigate the above issue by extending the theory of partial distinguishability [6, 19] to the case of photodetection with precise time resolution. In doing this, we account for *realistic* single photons in mixed states, in contrast to related Refs. [21, 23], applicable only to *pure-state* photons. Pure-state photons, however, are not available in experiments [29]. For instance, the standard spontaneous parametric down-conversion sources of single photons [30, 31] as well as the quantum dot sources [32] lead to random emission times (for instance, in the former case only a “thermal-difference” mixed state of single photon can be achieved [33]). Additionally, realistic detectors act by projection onto mixed states [34, 35], with probabilities of outcomes given by positive-operator valued measures. We use mixed-state single photons with random arrival times to model such sources of noise in experiments. Single photons with near-unity purity/indistinguishability have been recently experimentally demonstrated [36, 37]. It remains to establish if the achieved purity is good enough for a large number $N \sim 50$ of photons [38], required for quantum advantage with boson sampling.

To better understand the effect of photon distinguishability due to mixed states in case of photodetection with precise time resolution, we compare with the well-studied case of photodetection incapable of (or with strongly imprecise) time resolution, first considered in Ref. [6]. Thus, we compare distinguishability in two setups of experimental boson sampling with single photons: (a) the standard setup, with photons of the same central frequency on a spatial interferometer with photodetection incapable of time resolution (slow detectors as compared to pulse duration of photons) and (b) that with photons of generally different central frequencies on the same spatial interferometer and photodetection with precise time

resolution (fast detectors). Our approach is applicable to any mixed states of photons, however, for explicit analytical results we use Gaussian-shaped photons with Gaussian distributed emission times.

We also generalize previously considered measure [7] of quality of experimental boson sampling to the case of photodetection with precise time resolution. Our measure coincides with the total probability that bosons behave as completely indistinguishable particles. It turns out that the two considered setups correspond to *the same* value of this measure of distinguishability.

The upshot of our work is that the (overall) distinguishability due to impure (mixed) states of photons cannot be circumvented by any photodetection scheme, even if it is capable of photon state resolution. This means, for instance, that using photons of different frequencies and photodetection with strongly precise time resolution, as compared to photon pulse duration, will not allow for a better quality (i.e., closer to ideal) boson sampling in comparison with photons of the same frequency and photodetection with strongly imprecise time resolution.

The text is organized as follows. In section II we introduce our model of Gaussian single photons, briefly recall known facts on distinguishability of photons [6], directly applicable to our setup (a) of boson sampling, with photodetection incapable of time resolution, subsection II A, and then discuss the effect of photon distinguishability in setup (b) of boson sampling, with photodetection capable of precise time resolution, subsection II B. In section III we generalize to setup (b) a measure of quality of photon indistinguishability, introduced previously for setup (a), and compare the quality of approximation to the ideal boson sampling by the two setups. In concluding section IV we discuss implications of our results. Some mathematical details of derivations are relegated to appendices A and B.

II. TWO SETUPS OF BOSON SAMPLING: WITH AND WITHOUT PHOTON ARRIVAL TIME RESOLUTION BY DETECTORS

We consider two setups of boson sampling with single photons on the same spatial interferometer, with and without photon arrival time resolution by detectors, respectively, panels (a) and (b) of figure 1, where in setup (a) single photons have the same central frequency, whereas in setup (b) they have, in general, different central frequencies. We assume that a unitary linear spatial interferometer, with M input and output ports, has all paths of equal optical length (independent of the frequency range of photons). Such an interferometer can be described by a unitary transformation between the M input and output spatial modes (ports)

$$\hat{a}_k^\dagger(t) = \sum_{l=1}^M U_{kl} \hat{b}_l^\dagger(t), \quad (1)$$

where U is a unitary matrix, and $\hat{a}_k(t)$ and $\hat{b}_k(t)$ are boson creation operators of the input and output ports at time t . Let us fix the input ports of single photons to be $k = 1, \dots, N$.

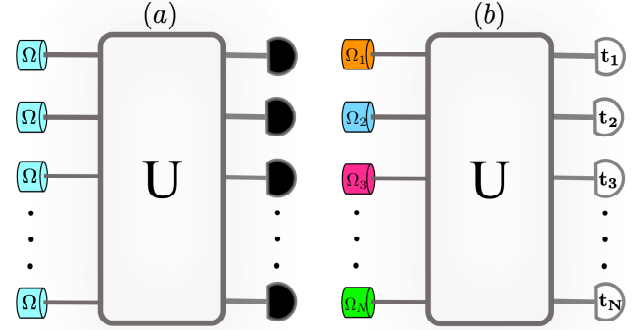


FIG. 1: A schematic depiction of our two setups of boson sampling with single photons: (a) N photons of the same central frequency Ω interfere on a unitary spatial M -port interferometer U and are detected at output ports without photodetection times resolution (slow detectors), with the output data being l_1, \dots, l_N (order is irrelevant); (b) N photons of frequencies $\Omega_1, \Omega_2, \dots, \Omega_N$ interfere on the same spatial interferometer U and are detected with precise resolution of photodetection times, with the output data being $(l_1, t_1), \dots, (l_N, t_N)$. In general $N \leq M$ and $l_k = l_j$ and/or $t_k = t_j$ for some $k \neq j$.

Our principal results and conclusions apply for general (mixed) states $\hat{\rho}_1, \dots, \hat{\rho}_N$ of input photons, however, we illustrate the approach by utilizing the simplest Gaussian model, where each photon has a Gaussian shape and arrival times also being distributed according to a Gaussian. Besides allowing explicit analytical results, the Gaussian-shaped single photons are optimal for multi-photon interference experiments [39]. Thus, we consider N single photons in the following mixed states:

$$\begin{aligned} \hat{\rho}_k &= \int d\tau p_k(\tau) |\Phi_{k,\tau}\rangle \langle \Phi_{k,\tau}|, \quad p_k(\tau) = \frac{1}{\sqrt{\pi} \Delta \tau_k} e^{-\frac{\tau^2}{\Delta \tau_k^2}} \\ |\Phi_{k,\tau}\rangle &= \int dt \Phi_{k,\tau}(t) \hat{a}_k^\dagger(t) |0\rangle \\ \Phi_{k,\tau}(t) &= \frac{1}{\pi^{1/4} \sqrt{T_k}} \exp\left(-i\Omega_k t - \frac{(t-\tau)^2}{2T_k^2}\right), \end{aligned} \quad (2)$$

where $\Delta \tau_k$ is the standard deviation of arrival time of photon k , T_k is the temporal width of the photon pulse, and Ω_k is its central frequency. In Eq. (2) we have assumed that the Gaussian distributed arrival times of photons have the same average ($\bar{\tau} = 0$), since our main objective is to study the effect of randomness (in photon arrival times) on partial distinguishability of photons in the two setups of figure 1. On the other hand, constant bias in the average arrival times of single photons can be compensated for with delay lines. Photons in panels (a) and (b) of figure 1 differ in central frequency in Eq. (2):

in setup (a) photons have the same central frequency $\Omega_k = \Omega$, whereas in setup (b) central frequencies are generally different, $\Omega_k \neq \Omega_l$ for $k \neq l$.

A. Setup (a): no time resolution by detectors

Here we briefly recall the partial distinguishability theory [6, 19] directly applicable to setup (a) of figure 1. We also give an explicit expression for the distinguishability function of our Gaussian model and an exponential approximation (see Eqs. (12) and (14) below), which are new results. We therefore set the same central frequency $\Omega_k = \Omega$ in Eq. (2). Photodetection without arrival time resolution is described by the following positive operator valued measure (POVM) [6]

$$\hat{\Pi}_{\mathbf{m}} = \frac{1}{\mathbf{m}!} \int dt_1 \dots \int dt_N \prod_{k=1}^N \hat{b}_{l_k}^\dagger(t_k) |0\rangle\langle 0| \prod_{k=1}^N \hat{b}_{l_k}(t_k), \quad (3)$$

where $\mathbf{m} = (m_1, \dots, m_M)$ is an output configuration of photons, $m_1 + \dots + m_M = N$, m_l is the number of photons in output port l , l_1, \dots, l_N is a multi-set (i.e., with repetitions) of output ports, and $\mathbf{m}! = m_1! \dots m_M!$. The probability $\tilde{p}_{\mathbf{m}}$ of a given output configuration \mathbf{m} is

$$\tilde{p}_{\mathbf{m}} = \text{Tr}\{\hat{\Pi}_{\mathbf{m}} \hat{\rho}_1 \otimes \dots \otimes \hat{\rho}_N\}. \quad (4)$$

To compute the probability, we observe that Eq. (1) leads to the following identity [6]

$$\langle 0 | \left[\prod_{i=1}^N \hat{b}_{l_i}(t_i) \right] \prod_{j=1}^N \hat{a}_k^\dagger(t'_j) |0\rangle = \sum_{\sigma} \prod_{k=1}^N U_{\sigma(k), l_k} \delta(t'_k - t_{\sigma^{-1}(k)}), \quad (5)$$

where σ is a permutation of N objects. Identity (5) allows straightforward computation of the inner products involving boson operators in Eq. (4). In particular, to each term $|\Phi_{k, \tau_k}\rangle\langle\Phi_{k, \tau_k}|$ in the expansion of mixed state $\hat{\rho}_k$ of photon k in Eq. (2) corresponds the following inner product (and a similar conjugated one)

$$\begin{aligned} & \int dt'_1 \dots \int dt'_N \langle 0 | \left[\prod_{k=1}^N b_{l_k}(t_k) \right] \prod_{k=1}^N \Phi_{k, \tau_k}(t'_k) a_k^\dagger(t'_k) |0\rangle \\ &= \sum_{\sigma} \prod_{k=1}^N U_{\sigma(k), l_k} \Phi_{k, \tau_k}(t_{\sigma^{-1}(k)}). \end{aligned} \quad (6)$$

The probability $\tilde{p}_{\mathbf{m}}$ becomes [6, 19]

$$\tilde{p}_{\mathbf{m}} = \frac{1}{\mathbf{m}!} \sum_{\sigma_1, \sigma_2} J(\sigma_1 \sigma_2^{-1}) \prod_{k=1}^N U_{\sigma_1(k), l_k}^* U_{\sigma_2(k), l_k}, \quad (7)$$

with a distinguishability function $J(\sigma)$, given in this case by

$$J(\sigma) = \text{Tr}(P_{\sigma}^\dagger \rho_1 \otimes \dots \otimes \rho_N), \quad (8)$$

where we have used the unitary operator representation P_{σ} ($P_{\sigma}^\dagger = P_{\sigma^{-1}}$) of permutation σ , defined by

$$P_{\sigma} |x_1\rangle \otimes \dots \otimes |x_N\rangle = |x_{\sigma^{-1}(1)}\rangle \otimes \dots \otimes |x_{\sigma^{-1}(N)}\rangle, \quad (9)$$

and introduced the internal state ρ_k of photon k (observe that $\rho_k \neq \hat{\rho}_k$), defined as follows

$$\begin{aligned} \rho_k &\equiv \int dt \tau p_k(\tau) |\phi_{k, \tau}\rangle\langle\phi_{k, \tau}|, \quad |\phi_{k, \tau}\rangle = \int dt \phi_{k, \tau}(t) |t\rangle, \\ \phi_{k, \tau}(t) &= \frac{1}{\pi^{1/4} \sqrt{T_k}} \exp\left(-\frac{(t-\tau)^2}{2T_k^2}\right), \end{aligned} \quad (10)$$

where $|t\rangle$ is the time-basis state $\langle t|t'\rangle = \delta(t-t')$ and $p_k(\tau)$ is given by Eq. (2) (note that $\Phi_{k, \tau}(t) = e^{-i\Omega_k t} \phi_{k, \tau}(t)$).

Identical mixed internal states: $\rho_k = \rho$

Distinguishability due to mixed internal states, e.g. as in Eq. (10), is similar to the usual pure-state-overlap distinguishability [4], e.g., for two photons with internal states ρ_1 and ρ_2 the average absolute-value squared overlap of their states is $\text{Tr}(\rho_1 \rho_2)$. However, differently from the pure-state distinguishability, taking two photons in the same mixed internal state $\rho_{1,2} = \rho$ does not make them indistinguishable, since $\text{Tr}(\rho^2) \neq 1$. Therefore, to understand the effect of distinguishability due to mixed states of photons, it is sufficient to focus on the simplest case of photons in the same mixed internal state. Thus, for specific calculations, we will use $\Delta\tau_k = \Delta\tau$ and $T_k = T$ (see Eqs. (2) and (10), so that $\rho_k = \rho$, for all $k = 1, \dots, N$). In this case, the expression for distinguishability function $J(\sigma)$ of Eq. (8) simplifies considerably [6, 19]:

$$J(\sigma) = \prod_{n=2}^N \text{Tr}(\rho^n)^{C_n(\sigma)}, \quad (11)$$

where $C_n(\sigma)$ is the number of permutation cycles of length n , i.e., $i_1 \rightarrow i_2 \rightarrow \dots \rightarrow i_n \rightarrow i_1$, in the cycle decomposition of permutation σ (for more information see Ref. [40]). The higher-order purities $\text{Tr}(\rho^n)$ for $n = 2, \dots, N$ govern partial distinguishability of N single photons in the same (mixed) internal state ρ . For the Gaussian model of Eq. (10), moreover, the purities can be evaluated explicitly, as this amounts to evaluating multidimensional Gaussian integrals. We get from Eqs. (8) and (10) for $n \geq 2$

$$\begin{aligned}
\text{Tr}(\rho^n) &= \int d\tau_1 p(\tau_1) \dots \int d\tau_n p(\tau_n) \prod_{j=1}^n \langle \phi_{j,\tau_j} | \phi_{j+1,\tau_{j+1}} \rangle \\
&= \frac{1}{(\pi \Delta \tau^2)^{n/2}} \int d\tau_1 \dots \int d\tau_n \exp \left(-\frac{\sum_{j=1}^n \tau_j^2}{\Delta \tau^2} - \frac{\sum_{j=1}^n (\tau_j - \tau_{j+1})^2}{4T^2} \right) = \frac{1}{\sqrt{\det A}} \\
&= \prod_{j=0}^{n-1} \left[1 + \frac{\Delta \tau^2}{T^2} \sin^2 \left(\frac{\pi j}{n} \right) \right]^{-\frac{1}{2}}, \tag{12}
\end{aligned}$$

where index $j + n$ equivalent to j . We have used that the quadratic form in the exponent, in variables $\frac{\tau_j}{\Delta \tau}$, corresponds to a circulant matrix A with the only nonzero elements being $A_{jj} = 1 + \frac{\Delta \tau^2}{2T^2}$ and $A_{j,j \pm 1} = -\frac{\Delta \tau^2}{4T^2}$, whose determinant is given by an explicit analytical expression [41] (for more details, see appendix A).

Let us introduce the relative uncertainty in time of arrival by dividing the standard deviation of photon arrival time by its pulse duration $\eta \equiv \frac{\Delta \tau}{2T}$. When $\eta \rightarrow 0$ we get $\text{Tr}(\rho^n) = 1$ and thus $J(\sigma) = 1$, i.e., the ideal case of completely indistinguishable photons. For small $\eta \lesssim 0.125$, numerical evidence shows that the expression in Eq. (12) coincides with the following exponent

$$\text{Tr}(\rho^n) = \exp \left\{ -\frac{\eta^2 n}{\beta} \right\}, \quad n \geq 2, \tag{13}$$

with some slowly varying function $\beta = \beta(\eta, n) \approx 1$, see figure 2. Substituting approximation (13) into Eq. (11)

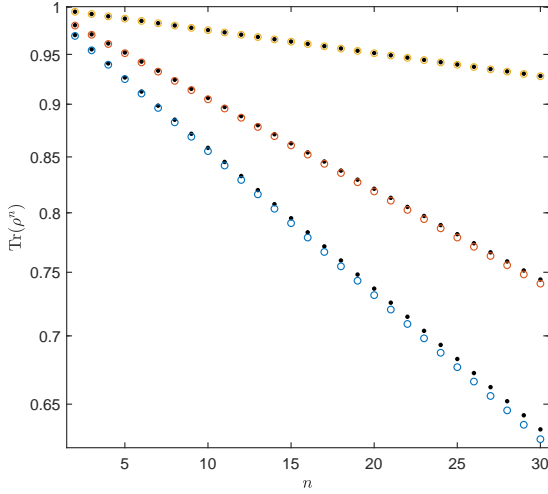


FIG. 2: Higher-order purity $\text{Tr}(\rho^n)$ (blobs) and its approximation by the exponent in Eq. (12) with $\beta = 1$ (circles) vs. n for several values of $\eta = \frac{\Delta \tau}{2T}$, from top to bottom: $\eta = 0.05; 0.1; 0.125$.

gives

$$J(\sigma) = \exp \left(-\frac{\eta^2}{\beta} [N - C_1(\sigma)] \right), \tag{14}$$

where we have used that the cycle lengths add up to N : $\sum_{n=1}^N n C_n(\sigma) = N$.

Rescaling the output probability of setup (a)

Below we will compare the output probability in two setups of figure 1. Setup (b) involves continuous basis of states in time (see the next section), with the usual problem of normalization for continuous bases. Instead of introducing an arbitrary countable state basis [42] for setup (b), it is more convenient (and sufficient) for our purpose to use directly the unnormalized symmetric basis states. For comparison of the two setups, we have to rescale the output probability of setup (a) in such a way that similar unnormalized symmetric basis states at the output are used, instead of the usual Fock states.

Let us rescale the output probability of Eq. (7) as follows $p_{\ell} \equiv \frac{\mathbf{m}!}{N!} \tilde{p}_{\mathbf{m}}$, where a multi-set of output ports $\ell = (l_1, \dots, l_N)$ corresponds to output configuration \mathbf{m} . Observe that, due to the summation identity for any symmetric function $f(l_1, \dots, l_N)$

$$\sum_{\mathbf{m}} f(l_1, \dots, l_N) = \sum_{l_1=1}^M \dots \sum_{l_N=1}^M \frac{\mathbf{m}!}{N!} f(l_1, \dots, l_N), \tag{15}$$

the normalization of probability $\sum_{\mathbf{m}} \tilde{p}_{\mathbf{m}} = 1$ becomes

$$\sum_{l_1=1}^M \dots \sum_{l_N=1}^M p_{\ell} = 1,$$

i.e., instead of occupation numbers \mathbf{m} (output configuration) the multi-set of output ports l_1, \dots, l_N is *formally* considered as the output data. From now on, we will also employ the superscript, (a) or (b), to distinguish the probability distributions of the two setups in figures 1(a) and 1(b). We obtain for the setup in figure 1(a)

$$\begin{aligned}
p_{\ell}^{(a)} &= \text{Tr} \{ \Pi_{\ell} \hat{\rho}_1 \otimes \dots \otimes \hat{\rho}_N \} \\
&= \frac{1}{N!} \sum_{\sigma_1, \sigma_2} J(\sigma_1 \sigma_2^{-1}) \prod_{k=1}^N U_{\sigma_1(k), l_k}^* U_{\sigma_2(k), l_k}, \tag{16}
\end{aligned}$$

with the POVM (compare with the Fock-state POVM $\hat{\Pi}_{\mathbf{m}}$ of Eq. (3))

$$\Pi_{\ell} = \frac{1}{N!} \int dt_1 \dots \int dt_N \prod_{k=1}^N \hat{b}_{l_k}^{\dagger}(t_k) |0\rangle\langle 0| \prod_{k=1}^N \hat{b}_{l_k}(t_k), \quad (17)$$

where $\frac{1}{\sqrt{N!}} \prod_{k=1}^N \hat{b}_{l_k}(t_k) |0\rangle$ is the mentioned above unnormalized symmetric basis state of N bosons. The POVM of Eq. (17) is positive semidefinite and normalized, since we have

$$\sum_{l_1=1}^M \dots \sum_{l_N=1}^M \Pi_{\ell} = \frac{1}{N!} \sum_{\sigma} P_{\sigma} \equiv S_N, \quad (18)$$

where S_N is the projector on the symmetric states of N particles, i.e., the identity operator in the Hilbert space of N bosons.

B. Setup (b): precise time resolution by detectors

Consider now the setup of figure 1(b) where, instead of introducing the actual detection time $\delta t \ll T$, for simplicity, we use the instantaneous detection model, thus we will consider probability density at output. The POVM density $\Pi_{\ell}(\mathbf{t})$, where $\mathbf{t} = (t_1, \dots, t_N)$, describing such a photodetection can be obtained from that of Eq. (17) by removing the integrals:

$$\Pi_{\ell}(\mathbf{t}) \equiv \frac{1}{N!} \left[\prod_{k=1}^N \hat{b}_{l_k}^{\dagger}(t_k) \right] |0\rangle\langle 0| \prod_{k=1}^N \hat{b}_{l_k}(t_k). \quad (19)$$

The output probability density $p_{\ell}(\mathbf{t})$ of detecting N input photons in the output ports ℓ at times \mathbf{t} is accordingly

$$p_{\ell}^{(b)}(\mathbf{t}) = \text{Tr}\{\Pi_{\ell}(\mathbf{t}) \hat{\rho}_1 \otimes \dots \otimes \hat{\rho}_N\}. \quad (20)$$

Similar as in the previous section, using the identity of Eq. (5) one can easily compute the inner products in Eq. (20) involving the boson creation and annihilation operators. By comparing of Eqs. (20) and (16) the derivation amounts to repetition of that of section II A with the integration over photodetection times removed and then rescaling the result. The following result is obtained

$$p_{\ell}^{(b)}(\mathbf{t}) = \frac{1}{N!} \sum_{\sigma_1, \sigma_2} \mathcal{J}(\mathbf{t}; \sigma_1, \sigma_2) \prod_{k=1}^N \mathcal{U}_{\sigma_1(k), l_k}^*(t_k) \mathcal{U}_{\sigma_2(k), l_k}(t_k),$$

$$\mathcal{U}_{k, l}(t) \equiv e^{-i\Omega_k t} U_{k, l}, \quad (21)$$

with the distinguishability function given as follows (compare with Eq. (8))

$$\begin{aligned} \mathcal{J}(\mathbf{t}; \sigma_1, \sigma_2) &= \prod_{k=1}^N \int d\tau_k p_k(\tau_k) \phi_{k, \tau_k}^*(t_{\sigma_1^{-1}(k)}) \phi_{k, \tau_k}(t_{\sigma_2^{-1}(k)}) \\ &= \text{Tr} (P_{\sigma_1}^{\dagger} |t_1\rangle\langle t_1| \otimes \dots \otimes |t_N\rangle\langle t_N| P_{\sigma_2} \rho_1 \otimes \dots \otimes \rho_N), \\ &= \prod_{k=1}^N \langle t_{\sigma_2(k)} | \rho_k | t_{\sigma_1(k)} \rangle \end{aligned} \quad (22)$$

where the inner state ρ_k of photon k is given in Eq. (10) and P_{σ} is defined in Eq. (9).

Note that the internal states of photons, i.e., the degrees of freedom that define the distinguishability functions in Eqs. (8) and (22), are the same and given by Eq. (10), i.e., irrespectively, whether we consider the setup with or without precise time resolution. Moreover, the following relation holds between the distinguishability functions of the two setups

$$\int dt_1 \dots \int dt_N \mathcal{J}(\mathbf{t}; \sigma_1, \sigma_2) = J(\sigma_1^{-1} \sigma_2). \quad (23)$$

Distinguishability function in the form similar to that of Eq. (22) has appeared before in discussion of the effect of state resolving photodetection on multiphoton interferences [27], however no analysis of partial distinguishability in such a setup was attempted before.

For input photons in pure states, i.e., for $\Delta\tau_k = 0$, the distinguishability function \mathcal{J} Eq. (22) factorizes as follows

$$\begin{aligned} \mathcal{J}(\mathbf{t}; \sigma_1, \sigma_2) &= \prod_{k=1}^N \phi_{k, 0}^*(t_{\sigma_1^{-1}(k)}) \phi_{k, 0}(t_{\sigma_2^{-1}(k)}) \\ &= \prod_{k=1}^N \phi_{\sigma_1(k), 0}^*(t_k) \phi_{\sigma_2(k), 0}(t_k) \end{aligned} \quad (24)$$

(in this case one has to set $\tau = 0$ in $\phi_{k, \tau}(t)$ of Eq. (10)). In this special case, using the relation $\Phi_{k, 0}(t) = e^{-i\Omega_k t} \phi_{k, 0}(t)$, one obtains

$$p_{\ell}^{(b)}(\mathbf{t}) = \frac{1}{N!} \left| \sum_{\sigma} \prod_{k=1}^N U_{\sigma(k), l_k}(t_k) \Phi_{\sigma(k), 0}(t_k) \right|^2, \quad (25)$$

i.e., the output probability is given by absolute value squared of a single matrix permanent of $U_{k, l} \Phi_{k, 0}(t_j)$. Thus, our approach reproduces the so-called “multiboson correlation sampling” with pure-state single photons [23]. In this case, the photons are completely indistinguishable (see also below). However, the states of photons in any experiment are mixed states due to various sources of noise, not allowing the factorization of \mathcal{J} as in Eq. (24).

When the distinguishability function in Eq. (22) satisfies $\mathcal{J}(\mathbf{t}; \sigma_1, \sigma_2) = 0$ whenever $\sigma_1 \neq \sigma_2$, there is no multiphoton interference, since the output probability is a convex combination of products of probabilities for each photon. Indeed, by Eq. (22) $0 \leq \mathcal{J}(\mathbf{t}; \sigma, \sigma) \leq 1$, whereas

$$p_{\ell}^{(b)}(\mathbf{t}) = \frac{1}{N!} \sum_{\sigma} \mathcal{J}(\mathbf{t}; \sigma, \sigma) \prod_{k=1}^N |U_{\sigma(k), l_k}(t_k)|^2. \quad (26)$$

The output probability density in Eq. (26) can be simulated with classical particles (which are classically indistinguishable). Therefore, it is the classical limit, in accordance with the theory [6, 19]. It occurs when the overlap between the different photon pulses vanishes, which in the model of Eq. (2) is the limit of infinite relative uncertainty in arrival times of photons $\Delta\tau_k/T_k \rightarrow \infty$.

Identical mixed internal states: $\rho_k = \rho$

In general, for different internal states of photons, $\rho_k \neq \rho_j$ for $k \neq j$, the distinguishability function \mathcal{J} of Eq. (22) depends on two permutations separately. However, as discussed in the previous section, it is sufficient to focus on photons in the same mixed internal state. When $\rho_k = \rho$ in Eq. (10) (i.e., $\Delta\tau_k = \Delta\tau$ and $T_k = T$) we get that \mathcal{J} of Eq. (22) depends only on the relative

permutation, $\mathcal{J}(\mathbf{t}; \sigma_1, \sigma_2) = \mathcal{J}(\mathbf{t}; \sigma_1 \sigma_2^{-1}, I)$ ($\sigma = I$ being the identity permutation) due to the following identities

$$P_{\sigma_2} \rho \otimes \dots \otimes \rho = \rho \otimes \dots \otimes \rho P_{\sigma_2}, \quad P_{\sigma_2} P_{\sigma_1}^\dagger = P_{\sigma_1 \sigma_2^{-1}}^\dagger. \quad (27)$$

Below we focus on this simplified case and use the notation $\mathcal{J}(\mathbf{t}; \sigma) \equiv \mathcal{J}(\mathbf{t}; \sigma, I)$. Evaluating Gaussian integrals in Eq. (22), we get

$$\mathcal{J}(\mathbf{t}; \sigma) = \frac{1}{(\pi[T^2 + \Delta\tau^2])^{N/2}} \exp \left(-\frac{\sum_{k=1}^N t_k^2}{T^2 + \Delta\tau^2} - \left(\frac{\Delta\tau}{2T} \right)^2 \frac{\sum_{k=1}^N (t_k - t_{\sigma(k)})^2}{T^2 + \Delta\tau^2} \right). \quad (28)$$

Only the second sum in the exponent in Eq. (28) depends on permutation σ . Thus, differently from $J(\sigma)$ of the previous section, we have $\mathcal{J}(\mathbf{t}, I) = p(\mathbf{t}) \neq 1$, where we have introduced the probability density $p(\mathbf{t})$ of detecting photons at times \mathbf{t} irrespective the output ports of a spatial interferometer U . Indeed, by unitarity of matrix U , we have from Eq. (21)

$$\begin{aligned} p(\mathbf{t}) &\equiv \sum_{l_1=1}^M \dots \sum_{l_M=1}^M p_{\ell}^{(b)}(\mathbf{t}) \\ &= \frac{1}{N!} \sum_{\sigma_1, \sigma_2} \mathcal{J}(\mathbf{t}; \sigma_1, \sigma_2) \prod_{k=1}^N \delta_{\sigma_1(k), \sigma_2(k)} e^{i(\Omega_{\sigma_1(k)} - \Omega_{\sigma_2(k)})t_k} \\ &= \frac{1}{N!} \sum_{\sigma} \mathcal{J}(\mathbf{t}; \sigma, \sigma) \stackrel{\rho_k \rightarrow \rho}{=} \mathcal{J}(\mathbf{t}, I), \end{aligned} \quad (29)$$

since for $\rho_k = \rho$ we have $\mathcal{J}(\mathbf{t}; \sigma, \sigma) = \mathcal{J}(\mathbf{t}; \sigma \sigma^{-1}, I) \equiv \mathcal{J}(\mathbf{t}; I)$ and there are exactly $N!$ permutations σ of N objects.

It is clear from Eqs. (26) and (29) that the probability density $p(\mathbf{t})$ is also the weight of the respective classical contribution to output probability density of detecting photons in output ports ℓ and times \mathbf{t} . Recall that in the setup of figure 1(a) the weight of the classical contribution to output probability is always $J(I) = 1$, by the normalization of the distinguishability function, Eq. (8). Therefore, to compare the distinguishability of photons in the two setups, for each given set of photodetection times \mathbf{t} in setup (b), we rescale $\mathcal{J}(\mathbf{t}; \sigma)$ so that the classical contribution is also weighted by 1. We therefore divide the distinguishability function $\mathcal{J}(\mathbf{t}; \sigma)$ of Eq. (28) by the probability density $p(\mathbf{t})$ of Eq. (29). Hence, the *proper distinguishability function* of setup (b) becomes

$$\begin{aligned} \tilde{\mathcal{J}}(\mathbf{t}; \sigma) &\equiv \frac{\mathcal{J}(\mathbf{t}; \sigma)}{p(\mathbf{t})} = \prod_{k=1}^N \frac{\langle t_k | \rho | t_{\sigma(k)} \rangle}{\langle t_k | \rho | t_k \rangle} \\ &= \exp \left(-\eta^2 \frac{\sum_{k=1}^N (t_k - t_{\sigma(k)})^2}{T^2 + \Delta\tau^2} \right) \end{aligned} \quad (30)$$

Introducing the following pure states

$$\chi_k(t) \equiv \frac{1}{(\pi[T^2 + \Delta\tau^2])^{1/4}} \exp \left(-i\Omega_k t - \frac{t^2}{2(T^2 + \Delta\tau^2)} \right), \quad (31)$$

(we have inserted the phase $e^{-i\Omega_k t}$ needed below when rewriting the output probability), from Eqs. (28) and (29) we get

$$p(\mathbf{t}) = \prod_{k=1}^N |\chi_k(t_k)|^2. \quad (32)$$

Now we can recast the probability density of Eq. (21) in the following form

$$\begin{aligned} p_{\ell}^{(b)}(\mathbf{t}) &= \frac{1}{N!} \sum_{\sigma_1, \sigma_2} \tilde{\mathcal{J}}(\mathbf{t}; \sigma_1 \sigma_2^{-1}) \prod_{k=1}^N \tilde{\mathcal{U}}_{\sigma_1(k), l_k}^*(t_k) \tilde{\mathcal{U}}_{\sigma_2(k), l_k}(t_k), \\ \tilde{\mathcal{U}}_{k, l}(t) &\equiv U_{k, l} \chi_k(t), \end{aligned} \quad (33)$$

where we have introduced a modified spatiotemporal matrix $\tilde{\mathcal{U}}_{k, l}(t_j)$.

For $\Delta\tau = 0$, i.e., photons in pure states, we get from Eq. (30) $\tilde{\mathcal{J}}(\mathbf{t}; \sigma) = 1$ and Eq. (33) reduces to the single permanent expression of Eq. (25) (in this case $\chi_k(t) = \phi_{k, 0}(t)$). In any experiment, however, mixed states of photons invariably lead to partial distinguishability with some nontrivial distinguishability function $\tilde{\mathcal{J}}(\mathbf{t}; \sigma)$ in Eq. (33), for our Gaussian model given by Eq. (30).

We already know from Eq. (23) that the proper distinguishability function $\tilde{\mathcal{J}}(\mathbf{t}; \sigma)$ averaged over $p(\mathbf{t})$ coincides with $J(\sigma)$. There is, moreover, an insightful similarity relation, in the functional dependence on σ , between the proper distinguishability functions of the two setups. Namely, the argument in the exponent in the case of $\tilde{\mathcal{J}}(\mathbf{t}; \sigma)$ Eq. (30), averaged over random photodetection times \mathbf{t} with the probability density $p(\mathbf{t})$ Eq. (32), gives $-\eta^2(N - C_1(\sigma))$, i.e., the argument in the exponent of $J(\sigma)$ (up to a slowly-varying denominator β) in

Eq. (14). Indeed, there are exactly $N - C_1(\sigma)$ nonzero average squared differences $\overline{(t_k - t_{\sigma(k)})^2}$ with the same value

$$\int dt_1 \int dt_2 |\chi(t_1)|^2 |\chi(t_2)|^2 (t_1 - t_2)^2 = T^2 + \Delta\tau^2.$$

The similarity of partial distinguishability of photons in the two setups reveals that distinguishability due to mixed states is not compensated for by increasing photodetection time resolution up to arbitrarily sharp resolution.

Note that the output probability formula given by Eqs. (31) and (33) corresponds a non-unitary transformation $\tilde{\mathcal{U}}_{k,l}(t_j)$ for any finite photon pulse width T . In contrast, the same probability density in the form of Eq. (21) has the desired unitarity feature of $\mathcal{U}_{k,l}(t_j)$, where the temporal part of the combined spatiotemporal “interferometer” is given by the Fourier transform. Thus, according to Eq. (21), photodetection with precise time of arrival resolution also performs a unitary transformation, additional to the one performed by a spatial interferometer. By doing this, it converts the running phases, $e^{-\Omega_k t}$, of photons into operating modes, in the terminology of Refs. [6, 19], thus they are not part of internal states in Eq. (10). This is reflected in the fact that (as we show in the next section) while the rescaled function $\tilde{\mathcal{J}}(\mathbf{t}; \sigma)$ of Eq. (30) is the proper distinguishability function, it is nevertheless the full function $\mathcal{J}(\mathbf{t}; \sigma)$ of Eq. (28) that governs the quality of boson sampling in the setup of figure 1(b).

III. MEASURE OF INDISTINGUISHABILITY AND QUALITY OF EXPERIMENTAL BOSON SAMPLING

Let us now quantify how partial distinguishability affects the quality of boson sampling in the two setups considered in the previous section, where the quality is measured by closeness to the ideal case with completely indistinguishable bosons. We employ the total variation distance, used in the analysis of computational complexity of boson sampling in Ref. [2], to judge how close is an experimental setup to the ideal case.

Previously, for the setup in figure 1(a), we have introduced a measure of closeness of an experimental realization of boson sampling with partially distinguishable bosons (and no other imperfections) to the ideal case, given by $1 - d_s$, where d_s is the projection of the internal state of bosons on the symmetric subspace (which corresponds to completely indistinguishable bosons [6, 19]). This measure serves as an upper bound on the respective total variation distance [7]. It was also argued in Ref. [7] that the bound must be tight, since d_s is the probability that the input bosons behave as completely indistinguishable. Below we extend the measure of Ref. [7] for the setup of figure 1(b) and compare the quality of experimental boson sampling in the two setups.

Let us now introduce the ideal case (i.e., with completely indistinguishable bosons) of the two setups of boson sampling by setting $J(\sigma) = 1$ in Eq. (16) and $\tilde{\mathcal{J}}(\mathbf{t}, \sigma) = 1$ in Eq. (33). Let us denote the probabilities (probability density for setup (b)) in the ideal case by $\mathring{p}_{\ell}^{(a)}$ and $\mathring{p}_{\ell}^{(b)}(\mathbf{t})$, respectively. From Eq. (7) we get

$$\mathring{p}_{\ell}^{(a)} = \frac{1}{N!} \left| \sum_{\sigma} \prod_{k=1}^N U_{\sigma(k), l_k} \right|^2 = \frac{|\text{per}(U[1\dots N | l_1 \dots l_N])|^2}{N!}, \quad (34)$$

where $U[1\dots N | l_1 \dots l_N]$ is a submatrix of U on rows $1, \dots, N$ and columns l_1, \dots, l_N , and $\text{per}(\dots)$ stands for the matrix permanent. Similarly, setting $\tilde{\mathcal{J}}(\mathbf{t}; \sigma) = 1$ in Eq. (33) we obtain

$$\mathring{p}_{\ell}^{(b)}(\mathbf{t}) = \frac{|\text{per}(\tilde{\mathcal{U}}[1\dots N | (l_1, t_1) \dots (l_N, t_N)])|^2}{N!}, \quad (35)$$

where $\tilde{\mathcal{U}}[1\dots N | (l_1, t_1) \dots (l_N, t_N)]$ is a similar “submatrix” of $\tilde{\mathcal{U}}_{k,l}(t)$ of Eq. (33).

One comment is in order on Eq. (35). From the previous section we know that in the case of setup (b) photons in whatever pure states are completely indistinguishable. However, the output distribution of Eq. (33), for photons in mixed states, can approximate that of Eq. (35), for photons in pure states, only if in the latter case the same distribution $p(\mathbf{t})$ of detection times appears, Eq. (32), since $p(\mathbf{t})$ is independent of the proper distinguishability function $\tilde{\mathcal{J}}$. Therefore, in Eq. (35) we choose pure state of photon k to be $\chi_k(t)$ of Eq. (31) (with $\Delta\tau \neq 0$, in contrast to Eq. (25)), which guarantees the same $p(\mathbf{t})$.

Consider the total variation distance to the ideal case in the two setups:

$$\mathcal{D}^{(a)} = \frac{1}{2} \sum_{l_1=1}^M \dots \sum_{l_N=1}^M |p_{\ell}^{(a)} - \mathring{p}_{\ell}^{(a)}|, \quad (36)$$

$$\mathcal{D}^{(b)} = \frac{1}{2} \int dt_1 \dots \int dt_N \sum_{l_1=1}^M \dots \sum_{l_N=1}^M |p_{\ell}^{(b)}(\mathbf{t}) - \mathring{p}_{\ell}^{(b)}(\mathbf{t})|. \quad (37)$$

On the right hand side in Eqs. (36) and (37) we have rescaled probabilities of Eq. (16) and (20), where output ports ℓ (and also photodetection times \mathbf{t}) appear in the summations (integrals) instead of Fock state occupations. The output probability of setup (a) is symmetric in ℓ and that of setup (b) in (ℓ, \mathbf{t}) , thus permutations of ℓ ((ℓ, \mathbf{t})) do not change the probabilities. Since, moreover, both distributions are appropriately rescaled, Eqs. (36)-(37) correctly give the total variation distance. For instance, in the case of setup (a) by combining all the possible sequences of output ports ℓ corresponding to the same output configuration \mathbf{m} and using the summation identity of Eq. (15) we get

$$\sum_{l_1=1}^M \dots \sum_{l_N=1}^M |p_{\ell}^{(a)} - \mathring{p}_{\ell}^{(a)}| = \sum_{\mathbf{m}} |\tilde{p}_{\mathbf{m}} - \tilde{p}_{\mathbf{m}}|,$$

where $\tilde{p}_{\mathbf{m}}$ is the probability given in Eq. (7) and $\mathring{p}_{\mathbf{m}}^{(a)}$ is the respective probability in the ideal case.

In Ref. [7], for the model of identical internal states $\rho_k = \rho$ it was shown that

$$\mathcal{D}^{(a)} \leq 1 - d_s, \quad d_s = \text{Tr}(S_N \rho \otimes \dots \otimes \rho) = \frac{1}{N!} \sum_{\sigma} J(\sigma). \quad (38)$$

where S_N is defined in Eq. (18). We remind here that d_s defined in Eq. (38) is the probability that internal state of N single photons, $\rho \otimes \dots \otimes \rho$, is a state of N completely indistinguishable photons, in this case

$$\mathring{\rho} \equiv \frac{S_N \rho \otimes \dots \otimes \rho S_N}{d_s}, \quad (39)$$

since S_N is a projector on a symmetric state. Therefore, d_s gives also a measure of how indistinguishable bosons are in an experimental setup (more details in Ref. [7]).

Now let us find an equivalent measure, which replaces d_s of Eq. (38), in the case of setup of figure 1(b). To find the measure, let us generalize the derivation of the upper bound in Eq. (38) to setup (b). The probability of Eq. (33) as compared to that of Eq. (16) has one essential new feature: dependence of the distinguishability function $\tilde{\mathcal{J}}$ on the output data (photodetection times \mathbf{t}). Notwithstanding this fact, the main idea of Ref. [7] applies also to setup (b): we recast the output probability in a form where the distinguishability function serves as a “state” in some auxiliary linear space spanned by $N!$ permutations, whereas the spatial interferometer U and photodetection combine to a corresponding POVM in that linear space. This simple trick not only allows us to derive a bound on the total variation distance $\mathcal{D}^{(b)}$ of Eq. (37), similar to that of Eq. (38), but also to find the measure of quality of boson sampling for setup (b) equivalent to that for setup (a).

Let us introduce an auxiliary linear space spanned by $N!$ basis vectors $|\sigma\rangle$, where one vector is introduced for each permutation σ of N objects. Next, we introduce a “state” (more precisely, state density) corresponding to the distinguishability function $\tilde{\mathcal{J}}(\mathbf{t}; \sigma)$ Eq. (30) which depends on detection times \mathbf{t} :

$$\langle \sigma_1 | \mathbf{J}(\mathbf{t}) | \sigma_2 \rangle \equiv \frac{1}{N!} \tilde{\mathcal{J}}(\mathbf{t}; \sigma_1 \sigma_2^{-1}). \quad (40)$$

The distinguishability function $\tilde{\mathcal{J}}(\mathbf{t}; \sigma)$ Eq. (30) is a positive-semidefinite function over permutations, i.e., for any complex-valued function $z(\sigma)$ we have

$$\begin{aligned} & \sum_{\sigma_1, \sigma_2} \tilde{\mathcal{J}}(\mathbf{t}; \sigma_1 \sigma_2^{-1}) z(\sigma_1) z^*(\sigma_2) \\ &= \prod_{k=1}^N \sum_{\sigma_1, \sigma_2} z^*(\sigma_2) \frac{\langle t_{\sigma_2(k)} | \rho | t_{\sigma_1(k)} \rangle}{\langle t_k | \rho | t_k \rangle} z(\sigma_1) \geq 0. \end{aligned}$$

Therefore, the introduced operator in Eq. (40) is a positive semi-definite operator in the auxiliary linear space,

normalized as follows

$$\text{tr}(\mathbf{J}(\mathbf{t})) \equiv \langle \sigma | \mathbf{J}(\mathbf{t}) | \sigma \rangle = 1. \quad (41)$$

Next, we introduce rank-1 POVM on vectors $|Z_{\ell}(\mathbf{t})\rangle$ in the auxiliary linear space, where

$$\langle \sigma | Z_{\ell}(\mathbf{t}) \rangle \equiv \prod_{k=1}^N \tilde{\mathcal{U}}_{\sigma(k), l_k}(t_k), \quad (42)$$

with $\tilde{\mathcal{U}}_{k, l}(t)$ from Eq. (33). The probability density of Eq. (33) becomes an average in the auxiliary linear space,

$$p_{\ell}^{(b)}(\mathbf{t}) = \langle Z_{\ell}(\mathbf{t}) | \mathbf{J}(\mathbf{t}) | Z_{\ell}(\mathbf{t}) \rangle. \quad (43)$$

In the ideal case, i.e., with $\tilde{\mathcal{J}}(\mathbf{t}; \sigma) = 1$, Eq. (40) tells us that the corresponding auxiliary “state” is a projector

$$\mathring{\mathbf{J}}(\mathbf{t}) = |S\rangle\langle S|, \quad \langle \sigma | S \rangle = \frac{1}{\sqrt{N!}}. \quad (44)$$

The key observation for below derivation is that the “state” $\mathbf{J}(\mathbf{t})$ of Eq. (40) has $|S\rangle$ of Eq. (44) as an eigenvector, as can be easily established by verification using the definition. We have therefore

$$\mathbf{J}(\mathbf{t}) = \lambda(\mathbf{t}) |S\rangle\langle S| + (1 - \lambda(\mathbf{t})) \mathbf{J}^{(\perp)}(\mathbf{t}), \quad (45)$$

where

$$\lambda(\mathbf{t}) = \langle S | \mathbf{J}(\mathbf{t}) | S \rangle = \frac{1}{N!} \sum_{\sigma} \tilde{\mathcal{J}}(\mathbf{t}; \sigma) \leq 1 \quad (46)$$

where a positive semi-definite operator $\mathbf{J}^{(\perp)}(\mathbf{t})$ is normalized by $\text{tr}(\mathbf{J}^{(\perp)}(\mathbf{t})) = 1$ and satisfies the orthogonality condition $\mathbf{J}^{(\perp)}(\mathbf{t}) |S\rangle = \langle S | \mathbf{J}^{(\perp)}(\mathbf{t}) = 0$.

Note that due to our specific choice of the ideal case in Eq. (35) with $\chi_k(t)$ of Eq. (31), all the introduced “states” in the auxiliary linear space give the same probability density $p(\mathbf{t})$, given by Eq. (32). Indeed, in the ideal case, by repeating the calculation of Eq. (29) for $p_{\ell}^{(b)}(\mathbf{t})|_{\lambda(\mathbf{t})=1} = \mathring{p}_{\ell}^{(b)}(\mathbf{t})$, we get

$$\sum_{l_1=1}^M \dots \sum_{l_N=1}^M \mathring{p}_{\ell}^{(b)}(\mathbf{t}) = \prod_{k=1}^N |\chi_k(t_k)|^2. \quad (47)$$

From Eq. (45) we obtain the same result for the probability density $p_{\ell}^{(b)}(\mathbf{t})|_{\lambda(\mathbf{t})=0}$ corresponding to the “state” $\mathbf{J}^{(\perp)}(\mathbf{t})$. Hence, the same holds for $p_{\ell}^{(b)}(\mathbf{t})|_{\lambda(\mathbf{t})=f(\mathbf{t})}$ with any non-negative function $f(\mathbf{t}) \leq 1$, e.g., for the probability $p_{\ell}^{(b)}(\mathbf{t})|_{\lambda(\mathbf{t})=1/2}$ corresponding to the state $\frac{1}{2} (|S\rangle\langle S| + \mathbf{J}^{(\perp)}(\mathbf{t}))$. This important fact will be used below.

Rewriting the total variation distance of Eq. (37) in the introduced notations, we obtain

$$\begin{aligned}
\mathcal{D}^{(b)} &= \frac{1}{2} \int dt_1 \dots \int dt_N \sum_{l_1=1}^M \dots \sum_{l_N=1}^M \left| \langle Z_{\ell}(\mathbf{t}) | \hat{\mathbf{J}}(\mathbf{t}) - \mathbf{J}(\mathbf{t}) | Z_{\ell}(\mathbf{t}) \rangle \right| \\
&= \frac{1}{2} \int dt_1 \dots \int dt_N (1 - \lambda(\mathbf{t})) \sum_{l_1=1}^M \dots \sum_{l_N=1}^M \left| \langle Z_{\ell}(\mathbf{t}) | (|S\rangle\langle S| - \mathbf{J}^{(\perp)}(\mathbf{t})) | Z_{\ell}(\mathbf{t}) \rangle \right| \\
&\leq \int dt_1 \dots \int dt_N (1 - \lambda(\mathbf{t})) \sum_{l_1=1}^M \dots \sum_{l_N=1}^M \langle Z_{\ell}(\mathbf{t}) | \frac{1}{2} (|S\rangle\langle S| + \mathbf{J}^{(\perp)}(\mathbf{t})) | Z_{\ell}(\mathbf{t}) \rangle \\
&= \int dt_1 \dots \int dt_N (1 - \lambda(\mathbf{t})) \sum_{l_1=1}^M \dots \sum_{l_N=1}^M p_{\ell}^{(b)}(\mathbf{t}) |_{\lambda(\mathbf{t})=\frac{1}{2}} = \int dt_1 \dots \int dt_N (1 - \lambda(\mathbf{t})) p(\mathbf{t}) \\
&= 1 - \frac{1}{N!} \sum_{\sigma} \int dt_1 \dots \int dt_N \mathcal{J}(\mathbf{t}; \sigma) = 1 - d_s,
\end{aligned} \tag{48}$$

where we have used that $\frac{1}{2} (|S\rangle\langle S| + \mathbf{J}^{(\perp)}(\mathbf{t}))$ is positive semi-definite operator in the auxiliary linear space corresponding to $\lambda(\mathbf{t}) = 1/2$ in Eq. (45), have taken into account the above discussed fact that $p_{\ell}^{(b)}(\mathbf{t})|_{\lambda(\mathbf{t})=1/2} = p(\mathbf{t})$, with $p(\mathbf{t})$ of Eq. (32), used the relations between the distinguishability functions \mathcal{J} , $\tilde{\mathcal{J}}$, and J , given by Eqs. (23) and (32), and the definition of d_s in Eq. (38).

Thus, for the setup in figure 1(b) we have obtained the same bound on the total variation distance to the ideal boson sampling as for the setup in figure 1(a). The physical reason for this is that in these two setups the (total) probability that the input photons are completely indistinguishable is *the same*. Let us show that d_s of Eq. (38) is also the total probability that photons are completely indistinguishable in the case of setup of figure 1(b). Indeed, given photodetection times \mathbf{t} , by the fact that the projector $|S\rangle\langle S|$ of Eq. (45) corresponds to the ideal case in setup (b) (similar as in setup (a) [7]), the conditional on \mathbf{t} probability density that photons in setup (b) are completely indistinguishable reads $d_s^{(b)}(\mathbf{t}) = \lambda(\mathbf{t})$, where $\lambda(\mathbf{t})$ is the eigenvalue of $\mathbf{J}(\mathbf{t})$ in Eq (45). This can be also established using the internal state, conditional on photodetection with given times \mathbf{t} , which is easily obtained by comparing Eqs. (8) and Eq. (39) with Eq. (22)

$$\begin{aligned}
d_s^{(b)}(\mathbf{t}) &\equiv \frac{\left[\prod_{k=1}^N \otimes \langle t_k | \right] S_N \rho \otimes \dots \otimes \rho S_N \left[\prod_{k=1}^N \otimes | t_k \rangle \right]}{p(\mathbf{t})} \\
&= \frac{\text{Tr} (S_N | t_1 \rangle \langle t_1 | \otimes \dots \otimes | t_N \rangle \langle t_N | S_N \rho \otimes \dots \otimes \rho)}{p(\mathbf{t})} \\
&= \frac{1}{N!} \sum_{\sigma} \frac{\mathcal{J}(\mathbf{t}; \sigma)}{p(\mathbf{t})} = \frac{1}{N!} \sum_{\sigma} \tilde{\mathcal{J}}(\mathbf{t}; \sigma) = \lambda(\mathbf{t}),
\end{aligned} \tag{49}$$

where we have used the definition of S_N (18) and Eq.

(46). The total probability is therefore

$$\begin{aligned}
d_s^{(b)} &\equiv \int dt_1 \dots \int dt_N p(\mathbf{t}) d_s^{(b)}(\mathbf{t}) \\
&= \frac{1}{N!} \sum_{\sigma} \int dt_1 \dots \int dt_N \mathcal{J}(\mathbf{t}; \sigma) = d_s,
\end{aligned} \tag{50}$$

by Eqs. (46) and (49), the relation between the distinguishability functions in Eq. (23) and the definition of d_s (38). Hence, the bound $1 - d_s$ in Eqs. (38) and (48) bears the same physical interpretation for both setups of figure 1.

Finally, how small the purity of single photons should be for a good quality experimental boson sampling? Our common upper bound $1 - d_s$ can give a sufficient purity. An explicit expression can be obtained with the use of the approximation of Eq. (14) for $\eta \lesssim 0.125$ i.e., $\beta = 1$ (see figure 2). We have

$$\begin{aligned}
d_s &= \exp(-\eta^2 N) \sum_{n=0}^N \frac{1}{n!} \left(e^{\eta^2} - 1 \right)^n \\
&= \exp(-\eta^2 N) \left(e^{\eta^2} + \sum_{n=2}^N \frac{1}{n!} \left(e^{\eta^2} - 1 \right)^n \right)
\end{aligned} \tag{51}$$

(see mathematical details in appendix B). For a given purity of single photons, $\mathcal{P} \equiv \text{Tr}(\rho^2) = e^{-2\eta^2}$, from Eq. (51) we get

$$\mathcal{D}^{(a,b)} \leq 1 - d_s = \mathcal{P}^{\frac{N-1}{2}} \left(1 + \sum_{n=2}^N \frac{\left(1 - \sqrt{\mathcal{P}} \right)^n}{n! \mathcal{P}^{\frac{n-1}{2}}} \right). \tag{52}$$

For illustration, to have up to 10% deviation from the ideal case of N -photon experimental boson sampling for $20 \leq N \leq 50$ photons our estimate necessitates the photon state purity $0.989 \leq \mathcal{P} \leq 0.996$.

IV. CONCLUSION

We have considered how partial distinguishability due to inevitable noise in an experimental setup affects two different realizations of boson sampling with single photons, the standard setup for boson sampling [2], with photons of the same central frequency on a spatial interferometer, and the so-called “multiboson correlation sampling” of Ref. [23], with photons of different central frequencies, in general. To be able to carry out all calculations explicitly, we have focused on the specific model of mixed-state input photons having Gaussian temporal shapes with random arrival times governed by a Gaussian distribution. Our main results bear clear physical interpretations, thus the conclusions are independent of the considered model.

We have found that the partial distinguishability theory of Refs. [6, 19] applies also to multiphoton interference with photodetection capable of precise time resolution, moreover, the output probability distribution is given by a similar mathematical expression as for the time-unresolved photodetection, where a function of permutations describes partial distinguishability of photons. For input photons in pure states, the output probability is given by the absolute value squared of a single matrix permanent, reproducing the results of Refs. [21, 23]. In this case photons are completely indistinguishable, since photodetection with precise time resolution turns the otherwise internal (temporal) states of photons into the operating modes by coherently mixing different paths of photons. Separation of degrees of freedom into the operating modes and the internal states is the prerequisite for application of the general theory of Refs. [6, 19]. We find that, while the average pure states of photons are operating modes under the photodetection with precise photon state resolution, the fluctuations about them are not, and the latter define the internal states of photons.

Whereas, given that operating modes and internal states are identified, the applicability of the theory of Refs. [6, 19] to photodetection with precise time resolution may not come as big surprise (though other views exist [21]), the striking similarity of distinguishability of photons due to mixed states under photodetection with and without precise time resolution and the same probability of photons to behave as completely indistinguishable in the two cases are rather surprising. These facts imply that purity of photons, usually reported alongside with photon distinguishability in current experiments, e.g., Refs. [36, 37], is in fact, the unavoidable distinguishability, whatever the photodetection scheme employed.

Though we have focused only on state-resolving photodetection where times of arrival are resolved by detectors, there is nothing special about the particular detection scheme considered. Our main results on distinguishability due to mixed states (noise) in an experimental setup are also applicable to frequency-resolved photodetection of photons with different times of arrival, as

for instance, in a recent experiment [43], with the roles played by time and frequency interchanged.

Finally, since the theory of Refs. [6, 19] is applicable to the case of photodetection with precise time (or frequency) resolution, all the previous results apply also to such setups as well, e.g., the fundamental limits on the quality of boson sampling experiments [6, 7] and the classical simulation algorithm, due to partial distinguishability [44]. We believe that this general conclusion provides a basis for assessment of experimental boson sampling setups with different detection schemes for demonstration of quantum advantage over digital computers.

V. ACKNOWLEDGEMENTS

V. S. was supported by the National Council for Scientific and Technological Development (CNPq) of Brazil, grant 307813/2019-3 and by the São Paulo Research Foundation (FAPESP), grant 2018/24664-9. M. E. O. B. was supported by the Coordenação de Aperfeiçoamento de Pessoal de Nível Superior (CAPES) of Brazil, Finance Code 001.

Appendix A: On derivation of Eq. (12)

Given a cyclic n -dimensional matrix A ,

$$A = \begin{pmatrix} a_0 & a_{n-1} & \dots & a_1 \\ a_1 & a_0 & \dots & a_2 \\ \vdots & \vdots & \ddots & \vdots \\ a_{n-1} & a_{n-2} & \dots & a_0 \end{pmatrix}, \quad (\text{A1})$$

introducing $\xi \equiv e^{\frac{2i\pi}{n}}$ we get [41]

$$\det A = \prod_{j=0}^{n-1} f(\xi^j), \quad f(x) \equiv a_0 + a_1 x + \dots + a_{n-1} x^{n-1}. \quad (\text{A2})$$

In case of matrix A in Eq. (12) we have only three non-zero elements: $a_0 = 1 + \frac{\Delta\tau^2}{2T^2}$ and $a_1 = a_{n-1} = -\frac{\Delta\tau^2}{4T^2}$. Using $\xi^{n-1} = \xi^{-1}$, we obtain

$$\begin{aligned} \det A &= \prod_{j=0}^{n-1} \left[1 + \frac{\Delta\tau^2}{2T^2} - \frac{\Delta\tau^2}{2T^2} \cos\left(\frac{2\pi j}{n}\right) \right] \\ &= \prod_{j=0}^{n-1} \left[1 + \frac{\Delta\tau^2}{T^2} \sin^2\left(\frac{\pi j}{n}\right) \right]. \end{aligned} \quad (\text{A3})$$

Appendix B: On derivation of Eq. (51)

We can use the method of generating function to compute the cycle sum Z_N in

$$d_s = \frac{1}{N!} \sum_{\sigma} \exp \left(-\frac{\eta^2}{\beta} [N - C_1(\sigma)] \right) = \exp \left(-\frac{\eta^2}{\beta} N \right) Z_N, \quad (\text{B1})$$

with $Z_N \equiv \frac{1}{N!} \sum_{\sigma} \zeta^{C_1(\sigma)}$ and $\zeta \equiv e^{\frac{\eta^2}{\beta}}$. Using that $\sum_{n=1}^N nC_n(\sigma) = N$ and [40]

$$\frac{1}{N!} \sum_{\sigma} (\dots) = \sum_{C_1, \dots, C_N} \frac{(\dots)}{\prod_{n=1}^N n^{C_n} C_n!}$$

we get the generating function $F(X) \equiv \sum_{N \geq 1} Z_N X^N$ as follows

$$\begin{aligned} F(X) &= \sum_{N \geq 1} \frac{1}{N!} \sum_{\sigma} (X\zeta)^{C_1(\sigma)} \prod_{n=2}^N X^{nC_n(\sigma)} \\ &= \sum_{C_1, \dots, C_N} \frac{(X\zeta)^{C_1} \prod_{n=2}^N X^{nC_n}}{\prod_{n=1}^N n^{C_n} C_n!} \\ &= \exp \left([\zeta - 1]X + \sum_{n=1}^{\infty} \frac{X^n}{n} \right) \\ &= \frac{\exp([\zeta - 1]X)}{1 - X}. \end{aligned} \quad (\text{B2})$$

Therefore

$$Z_N = \frac{1}{N!} \frac{d^N F(\zeta)}{d\zeta^N} \Big|_{\zeta=0} = \sum_{n=0}^N \frac{(\zeta - 1)^n}{n!}, \quad (\text{B3})$$

which results in the expression for d_s in Eq. (51) of section III.

[1] D. J. Brod, E. F. Galvão; A. Crespi, R. Osellame, N. Spagnolo and F. Sciarrino, *Advanced Photonics*, **1**, 034001 (2019).

[2] S. Aaronson and A. Arkhipov, arXiv:1011.3245 [quant-ph]; *Theory of Computing* **9**, 143 (2013).

[3] Hui Wang *et al*, *Phys. Rev. Lett.* **123**, 250503 (2019).

[4] C. K. Hong, Z. Y. Ou, and L. Mandel, *Phys. Rev. Lett.* **59**, 2044 (1987).

[5] P. P. Rohde and T. C. Ralph, *Phys. Rev. A* **85**, 022332 (2012).

[6] V. S. Shchesnovich, *Phys. Rev. A* **89**, 022333 (2014).

[7] V. S. Shchesnovich, *Phys. Rev. A* **91**, 063842 4 (2015).

[8] J. J. Renema, A. Menssen, W. R. Clements, G. Triginer, W. S. Kolthammer, and I. A. Walmsley, *Phys. Rev. Lett.* **120**, 220502 (2018).

[9] G. Kalai and G. Kindler, arXiv:1409.3093 [quant-ph].

[10] A. Leverrier and R. García-Patrón, arXiv:1309.4687 [quant-ph].

[11] A. Arkhipov, *Phys. Rev. A* **92**, 062326 (2015).

[12] S. Aaronson and D. J. Brod, *Phys. Rev. A* **93**, 012335 (2016).

[13] R. García-Patrón, J. J. Renema, and V. S. Shchesnovich, *Quantum* **3**, 169 (2019).

[14] M. Oszmaniec and D. J. Brod, *New J. Phys.* **20**, 092002 (2018).

[15] V. S. Shchesnovich, *Phys. Rev. A* **100**, 012340 (2019).

[16] M. C. Tichy, M. Tiersch, F. Mintert, and A. Buchleitner, *New Journal of Phys.* **14**, 093015 (2012).

[17] Y.-S. Ra, M. C. Tichy, H.-T. Lim, O. Kwon, F. Mintert, A. Buchleitner, and Y.-H. Kim, *PNAS* **110**, 1227 (2013).

[18] P. P. Rohde, *Phys. Rev. A* **91**, 012307 (2015).

[19] V. S. Shchesnovich, *Phys. Rev. A* **91**, 013844 (2015).

[20] M. C. Tichy, *Phys. Rev. A* **91**, 022316 (2015).

[21] V. Tamme and S. Laibacher, *Phys. Rev. Lett.* **114**, 243601 (2015).

[22] M. Tillmann, S.-H. Tan, S. E. Stoeckl, B. C. Sanders, H. de Guise, R. Heilmann, S. Nolte, A. Szameit, and P. Walther, *Phys. Rev. X* **5**, 041015 (2015).

[23] V. Tamme and S. Laibacher, *Quantum Inf. Process* **15**, 1241 (2016).

[24] J.-D. Urbina, J. Kuipers, S. Matsumoto, Q. Hummel, and K. Richter, *Phys. Rev. Lett.* **116**, 100401 (2016).

[25] M. Walschaers, J. Kuipers, and A. Buchleitner, *Phys. Rev. A* **94**, 020104(R) (2016).

[26] A. J. Menssen, A. E. Jones, B. J. Metcalf, M. C. Tichy, S. Barz, W. S. Kolthammer, and I. A. Walmsley, *Phys. Rev. Lett.* **118**, 153603 (2017).

[27] V. S. Shchesnovich and M. E. O. Bezerra, *Phys. Rev. A* **98**, 033805 (2018).

[28] A. E. Moylett and P. S. Turner, *Phys. Rev. A* **97**, 062329 (2018).

[29] M. E. Reimer and C. Cher, *Nat. Photonics* **13**, 734 (2019).

[30] W. P. Grice and I. A. Walmsley, *Phys. Rev. A* **56**, 1627 (1997).

[31] E. Meyer-Scott *et al*, *Phys. Rev. A* **95**, 061803(R) (2017).

[32] E. B. Flagg, S. V. Polyakov, T. Thomay, and G. S.

Solomon, Phys. Rev. Lett. **109**, 163601 (2012).

[33] D. Horoshko, S. De Biévre, G. Patera, and M. Kolobov, Phys. Rev. A **100**, 053831 (2019).

[34] S. M. Barnett, L. S. Phillips, and D. T. Pegg, Opt. Commun. **158**, 45 (1998).

[35] M. Ramilli, A. Allevi, V. Chmill, M. Bondani, M. Caccia, A. Andreoni, J. Opt. Soc. Am. B **27** 852 (2010).

[36] V. Ansari *et al*, Optics Express **26**, 2764 (2018).

[37] L. Dusanowski, S.-H. Kwon, C. Schneider, and S. Höfling, Phys. Rev. Lett. **122**, 173602 (2019).

[38] A. Neville, C. Sparrow, R. Clifford, E. Johnston, P. M. Birchall, A. Montanaro, A. Laing, Nature Physics **13**, 1153 (2017).

[39] P. P. Rohde, T. C. Ralph, and M. A. Nielsen, Phys. Rev. A **72**, 052332 (2005).

[40] R. P. Stanley, *Enumerative Combinatorics*, 2nd ed., Vol. 1 (Cambridge University Press, 2011).

[41] P. J. Davis, *Circulant Matrices* (American Mathematical Society; 2 edition 2012).

[42] K. J. Blow, R. Loudon, and S. J. D. Phoenix, Phys. Rev. A **42**, 4102 (1990).

[43] V. V. Orre, E. A. Goldschmidt, A. Deshpande, A.V. Gorshkov, V. Tamma, M. Hafezi, and S. Mittal, Phys. Rev. Lett. **123**, 123603 (2019).

[44] J. J. Renema, A. Menssen, W. R. Clements, G. Triginer, W. S. Kolthammer, and I. A. Walmsley, Phys. Rev. Lett. **120**, 220502 (2018).